Triggering role of acid sphingomyelinase in endothelial lysosome-membrane fusion and dysfunction in coronary arteries

Jun-Xiang Bao, Min Xia, Justin L. Poklis, Wei-Qing Han, Christopher Brimson and Pin-Lan Li

Am J Physiol Heart Circ Physiol 298:H992-H1002, 2010. First published 8 January 2010; doi:10.1152/ajpheart.00958.2009

AJP - Heart and Circulatory Physiology publishes original investigations on the physiology of the heart, blood vessels, and lymphatics, including experimental and theoretical studies of cardiovascular function at all levels of organization ranging from the intact animal to the cellular, subcellular, and molecular levels. It is published 12 times a year (monthly) by the American Physiological Society, 9650 Rockville Pike, Bethesda MD 20814-3991. Copyright © 2010 by the American Physiological Society. ISSN: 0363-6135, ESSN: 1522-1539. Visit our website at http://www.the-aps.org/.

Am J Physiol Heart Circ Physiol 298: H992–H1002, 2010.
First published January 8, 2010; doi:10.1152/ajpheart.00958.2009.

Triggering role of acid sphingomyelinase in endothelial lysosome-membrane fusion and dysfunction in coronary arteries

Jun-Xiang Bao, Min Xia, Justin L. Poklis, Wei-Qing Han, Christopher Brimson, and Pin-Lan Li

Department of Pharmacology and Toxicology, Medical College of Virginia, Virginia Commonwealth University, Richmond, Virginia

Submitted 13 October 2009; accepted in final form 2 January 2010

Bao JX, Xia M, Poklis JL, Han WQ, Brimson C, Li PL. Triggering role of acid sphingomyelinase in endothelial lysosome-membrane fusion and dysfunction in coronary arteries. *Am J Physiol Heart Circ Physiol* 298: H992–H1002, 2010. First published January 8, 2010; doi:10.1152/ajpheart.00958.2009.—The present study determined whether activation of acid sphingomyelinase (ASM) drives membrane proximal lysosomes to fuse to the cell surface, facilitating membrane lipid rafts (LRs) clustering in coronary arterial endothelial cells (CAECs) and leading to endothelial dysfunction. By confocal microscopy, the activators of ASM, phosphatidylinositol (PI), and bis (monoacylglyceryl) phosphate (Bis), and an inducer of ASM, butyrate, were found to increase LRs clustering in bovine CAECs, which was blocked by lysosome fusion inhibitor vacuolin-1. However, arsenic trioxide (Ars), an inducer of de novo synthesis of ceramide, had no such effect. Similarly, vacuolin-1-blockable effects were observed using fluorescence resonance energy transfer detection. Liquid chromatography-electrospray ionization-tandem mass spectrometry analysis demonstrated that all of these treatments, even Ars, increased ceramide production in CAECs. When ASM gene was silenced, all treatments except Ars no longer increased ceramide levels. Furthermore, dynamic fluorescence monitoring in live cells showed that PI and Bis stimulated lysosome-membrane fusion in CAECs. Functionally, PI and Bis impaired endothelium-dependent vasodilation in perfused coronary arteries, which was blocked by vacuolin-1 and a lysosome function inhibitor, bafilomycine. FasL (Fas ligand), a previously confirmed lysosome fusion stimulator as a comparison, also produced a similar effect. It is concluded that ASM activation serves as a triggering mechanism and driving force, leading to fusion of membrane proximal lysosomes into LR clusters on the cell membrane of CAECs, which represents a novel mechanism mediating endothelial dysfunction during death receptor activation or other pathological situation.

membrane microdomains; sphingolipids; acid vesicles; coronary circulation; vascular endothelium

LIPID RAFTS (LR) THAT CONSIST of dynamic assemblies of cholesterol, lipids with saturated acyl chains, such as sphingolipids and glycosphingolipids in the exoplasmic leaflet of the membrane bilayer, are now emerging as an important cellular signaling mechanism in the regulation of a variety of cell functions (1, 3, 13, 20, 24, 35, 41). It has been shown that clustered membrane LRs could form relatively large macrodomains, which serve to recruit or aggregate various receptors, such as tumor necrosis factor-α receptors, insulin receptors, or Fas, and also aggregate various signaling molecules, such as trimeric G proteins, sphingomyelin, tyrosine kinases, and phosphatases, resulting in activation of different signaling pathways (6, 9, 12, 27).

Address for reprint requests and other correspondence: P.-L. Li, Dept. of Pharmacology and Toxicology, Medical College of Virginia, Virginia Commonwealth Univ., 410 N 12th, Richmond, VA 23298 (e-mail: pli@vcu.edu).

Recent studies in our laboratory have indicated that LR clustering mediates the formation of membrane signaling platforms in response to death receptor activation in coronary arterial endothelial cells (CAECs). One of such signaling platforms was referred to as LR-redox signaling platforms, which was commented to be taking center stage in endothelial cell (EC) redox signaling pathway by editors of *Hypertension* (18–20, 40, 41). Over the last 2 yr, we have found that the LR-redox signaling was related to the increased activity of acid sphingomyelinase (ASM), which is a lysosomal glycoprotein and catalyzes the degradation of membrane-bound sphingomyelin into phosphocholine and ceramide (18, 19, 40). We have also reported that lysosomal vesicles may fuse to the cell membrane and play an important role in the formation of these signaling platforms during death receptor activation (19). However, the mechanism mediating this lysosome fusion and subsequent activation of redox signaling pathway has yet to be elucidated. In previous studies, some evidence was provided to suggest that ASM and its product ceramide may be importantly involved in intracellular moving or fusion of various organelles within different cells (11, 31). So far, it is unclear whether such ASM-mediated ceramide production also contributes to the fusion of lysosomes to the cell membrane. The present study was designed to test the hypothesis that ASM activation produces ceramide in lysosomes, which triggers and drives membrane proximal lysosome fusion to the cell surface, facilitating LR clustering on the membrane of ECs and ultimately resulting in endothelial dysfunction. We used two ASM activators, phosphatidylinositol (PI) and bis (monoacylglyceryl) phosphate (Bis), an ASM inducer, butyrate (Buty), and an activator of de novo synthesis of ceramide, arsenic trioxide (Ars), to activate or induce ASM and then observed lysosome moving and fusion. In addition, lysosome function inhibitor [bafilomycine (Baf)], fusion blocker (vacuolin-1), and ASM small interfering RNA (siRNA) were used to study lysosome behavior. By confocal microscopy, fluorescence resonance energy transfer (FRET) detection, liquid chromatography-electrospray ionization-tandem mass spectrometry (LC-ESI-MS-MS) analysis, and membrane fusion measurements, we demonstrated that it is the activation of ASM that triggers and drives membrane proximal lysosomes to move and fuse to EC membrane in LR-enriched area, thereby forming LR-lysosome signaling platforms and mediating transmembrane signaling.

MATERIALS AND METHODS

Cell culture. Bovine CAECs were isolated and maintained in RPMI 1640 (Invitrogen, Carlsbad, CA) containing 10% FBS (HyClone, Waltham, MA) and 1% antibiotics (Sigma, St. Louis, MO), as described previously (18–20, 40). All studies were performed by using CAECs of two to four passages.

Immunofluorescent microscopic analysis of LR clusters. CAECs were grown on poly-L-lysine-coated glass coverslips and treated with the following compounds, as described in different protocols: Fas ligand (FasL; 10 ng/ml, 15 min, Upstate, Bedford, MA), PI (5 μg/ml, 30 min, Sigma, St. Louis, MO), Bis (1 μg/ml, 30 min, Echelon, Salt Lake City, UT), Buty (500 μM, 20 h, Sigma), or Ars (1 μM, 20 h, Sigma), with or without pretreatment with vacuolin-1 (10 μM, 1 h, Sigma). LRs were detected with Alexa Fluor 488 conjugated cholera toxin B (Al488-CTXB, 2 μg/ml, 2 h, Molecular Probes, Carlsbad, CA) under a conventional Zeiss fluorescence microscope or a Olympus confocal microscope, as our laboratory described previously (18–20, 40, 41). The patch formation of Al488-CTXB and gangliosides complex represented the clusters of LRs. Clustering was defined as two or several intense patches of fluorescence on the cell surface, whereas unstimulated cells displayed a homogenous distribution of fluorescence throughout the membrane. In each experiment, the presence or absence of clustering in samples of 200 cells was scored by two independent observers. The results were given as the percentage of cells showing a cluster after the indicated treatment, as described in individual protocol.

RNA interference of ASM gene. The siRNA of ASM gene was purchased from QIAGEN, which has been proven to be efficient to knock down the ASM gene in CAECs by our laboratory's previous studies (20, 40) and was further confirmed in the present study (Supplemental Fig. 1). (The online version of this article contains supplemental data.) The DNA target sequence for this ASM-siRNA is 5′-AAGGCCGTGAGTTTCTACCT-3′. The scrambled small RNA (sRNA) (AATTCTCCGAACGTGTCACGT) was also confirmed as nonsilencing double-stranded RNA (40) and was used as control in the present study. Transfection of siRNA was performed using the QIAGEN TransMessenger transfection kit (Valencia, CA), according to the instruction manual.

LC-ESI-MS-MS analysis of ceramide. The production of ceramide was measured as described in our laboratory's previous studies (39) and by others (8, 32). Briefly, CAECs were grown on 10-cm dishes. After treatments with different compounds in various protocols, the cells were rinsed and harvested, followed by homogenation. Ten nanograms of C12 were added to homogenate reaction mixture containing 500 μg protein to act as an internal standard. Then the mixture was separated in chloroform/methanol/water (2:2:1.8). After evaporation with nitrogen and reconstitution with ethanol/formic acid (99.8:0.2), the samples were ready for LC-ESI-MS-MS assay. The separation of ceramide was performed on a Shumadzu SCL HPLC system (Kyoto, Japan) with a C18 Nucleosil AB Column (Macherey-Nagel, Duren, Germany). MS detection was carried out using an Applied Bio systems 3200 Q trap with a turbo V source for TurboIonSpray (Ontario, Canada). The concentrations of total ceramide, including C14, C16, C17, C18, and C20 ceramide, were calculated for statistics. The fragment ion obtained with the highest mass-to-charge ratio (*m/z* 264) was selected for quantitative MS detection in the multiple reaction monitoring mode (8).

FRET analysis of LRs with Lamp1. CAECs were first incubated with FITC-conjugated anti-Lamp1 antibody (a lysosomal marker protein, 1:200, BD Biosciences, San Jose, CA). Then the cells were incubated with tetramethylrhodamine isothiocyanate (TRITC)-conjugated CTXB (TRITC-CTXB, binds to the LR-enriched GM1 ganglioside, 2 μg/ml, 2 h, List Laboratories, Campbell, CA). The cells were visualized by confocal microscope. An acceptor bleaching protocol was employed to measure the FRET efficiency, as described in our laboratory's previous studies and by others (21, 22, 28, 33). After the prebleaching image was normally taken, the laser intensity at the excitement wavelength of the acceptor (TRITC) was increased from 50 to 98% and continued to excite the cell sample for 2 min to bleach the acceptor fluorescence. After the intensity of the excitement laser for acceptor was adjusted back to 50%, the postbleaching image was taken for FITC. A FRET image was obtained by subtraction of the prebleaching images from the postbleaching images and given a dark blue color. After measuring FITC fluorescence intensity of the pre-, post-, and FRET images, the FRET efficiency (E) was calculated through the following equation: E = (FITCpost − FITCpre)/FITCpost × 100%.

Confocal microscopic analysis of colocalization of Lamp1 with ASM or ceramide in CAECS. The CAECs were fixed with 4% paraformaldehyde in PBS for 10 min. Then some cells were permeabilized with 0.5% Tween 20 for 15 min. For detection of the colocalization of Lamp1 with ASM or ceramide, the CAECs were first incubated with FITC-labeled anti-Lamp1 antibody and then with rabbit anti-ASM polyclonal antibody (1:200, Santa Cruz, Santa Cruz, CA) or mouse anti-ceramide monoclonal antibody (1:1,000, Alexis Biochemicals, San Diego, CA), followed by incubation with Texas red (TR)-conjugated anti-rabbit or anti-mouse (1:500, Molecular Probes, Carlsbad, CA) secondary antibody, as needed. An excitation/emission wavelength of 570/625 nm was used for confocal microscopy of TR.

Quenching and dequenching of FM1–43 and destaining of FM2–10 in CAECs. For quenching experiments, after cells were loaded with 8 μM FM1–43 for 2 h, 1 mM bromide phenol blue (BPB) was added in the extracellular medium. For dequenching experiments, cells were loaded simultaneously with 8 μM FM1–43 and 1 mM BPB for 2 h. For destaining experiments, cells were loaded with 100 μM FM2–10 for 2 h. Then the CAECs were washed with FBS-free medium and a low power (λ excitation = 488 nm) of laser was used to scan cells. All of these experiments were used to detect lysosome fusion to the cell membrane, which was established in previous studies (16, 42).

Isolated small coronary artery tension recording. Fresh bovine hearts were obtained from a local abattoir. Small coronary arteries (~200 μm inner diameter) were dissected and stored in cell culture medium, which were then mounted in a Multi Myograph 610M (Danish Myo Technology, Aarhus, Denmark) for recording of their isometric wall tension, as described previously (4, 5). After 30 min of equilibration in physiological saline solution (pH 7.4) containing (in mM) 119 NaCl, 4.7 KCl, 1.6 $CaCl_2$, 1.17 $MgSO_4$, 1.18 NaH_2PO_4, 2.24 $NaHCO_3$, 0.026 EDTA, and 5.5 glucose, at 37°C, bubbled with a gas mixture of 95% O_2 and 5% CO_2, basic tension was set. Then the arteries were precontracted with a thromboxane A_2 analog, U-46619 (50 nM, Sigma). Once steady-state contraction was obtained, cumulative dose-response curves to the endothelium-dependent vasodilator bradykinin (BK, 10^{-10} to 10^{-6} M) were determined by measuring changes in wall tension. After being washed with physiological saline solution for 5 min three times, these arteries were pretreated by FasL (10 ng/ml for 20 min), PI (5 μg/ml for 40 min), or Bis (1 μg/ml for 40 min), with or without predisposal by Baf A1 (100 nM for 20 min, Sigma) or vacuolin-1 (10 μM for 1 h, Sigma), respectively. Then the contraction of artery to U-46619 and cumulative dose-response curves to BK were re-recorded.

Statistics. Data are presented as means ± SE. Significant differences between and within multiple groups were examined using ANOVA for repeated measures, followed by Duncan's multiple-range test. $P < 0.05$ was considered statistically significant.

RESULTS

LR clustering induced by FasL and activation of ASM. Figure 1*A* presents typical fluorescent microscopic images for LR clusters, as shown by an Al488-CTXB labeled fluorescent patch on the EC membrane. Under resting conditions (control), LRs were distributed over the EC membrane by weak, diffused green fluorescence. Stimulation of FasL, PI, Bis, Buty, but not Ars, led to the formation of green fluorescent patches in the EC membrane. Figure 1*B* summarizes the effects of different treatments on such LR clustering by counting positive cells with LR clusters or patches. Under resting condition, only

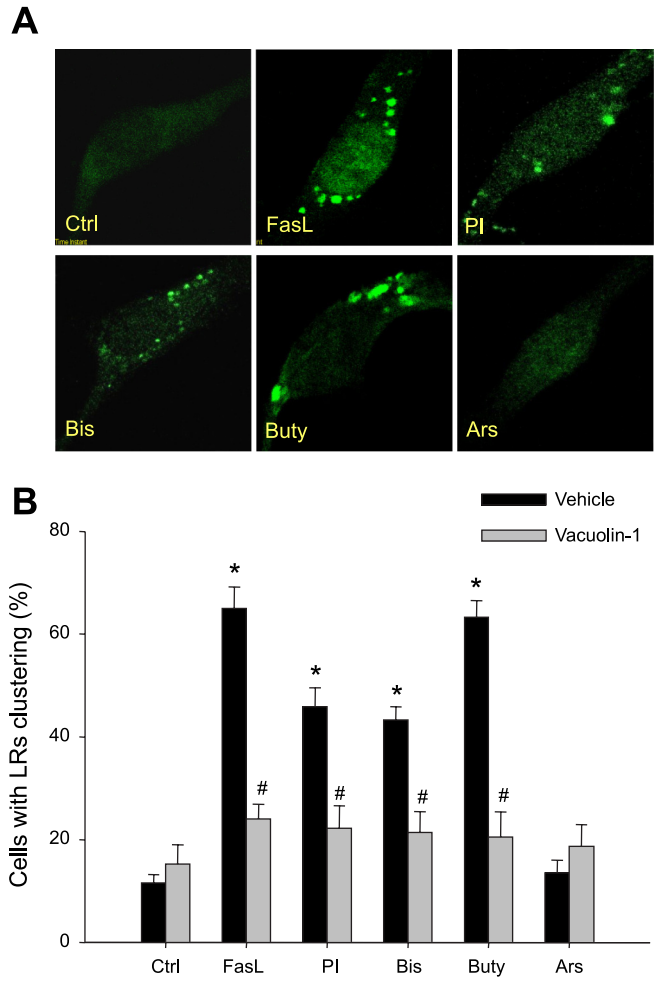

Fig. 1. *A*: representative images of lipid raft (LR) clustering in control (Ctrl) coronary artery endothelial cells (CAECs) and Fas ligand (FasL; 10 ng/ml for 15 min), phosphatidylinositol (PI; 5 μg/ml for 30 min), bis (monoacylglyceryl) phosphate (Bis; 1 μg/ml for 30 min), butyrate (Buty; 500 μM for 20 h), or arsenic trioxide (Ars; 1 μM for 20 h) stimulated cells. *B*: summarized results on percentage of cells with LR clustering in vehicle (Veh) or vacuolin-1 (10 μM for 1 h) pretreated group. Values are means ± SE; $n = 7$ batches of cells. $^{*}P < 0.05$ vs. Ctrl group. $^{\#}P < 0.05$ vs. respective Veh group.

11.6% of cells displayed positive LR clustering, whereas 65, 45.9, 43.3, and 63.3% of cells displayed such LR clustering after treatment with FasL, PI, Bis, and Buty, respectively. However, positive clustering in cells treated with Ars was not statistically significant compared with control cells. In the presence of vacuolin-1, an inhibitor of lysosome fusion to the cell membrane, LR clustering induced by FasL, PI, Bis, and Buty was almost completely blocked.

Ceramide production in CAECs with different treatments. Figure 2*A* shows the representative MS chromatography of ceramide from control and stimulated cells. Seven clear peaks corresponding to C12, C14, C16, C17, C18, C20, and C24 ceramides were detected. FasL as a positive control showed strong stimulatory action of ceramides, for almost all isoforms except C12 ceramide. Figure 2*B* summarizes the effects of different treatments on total ceramide production in CAECs. In vehicle and scramble sRNA-treated cells, all stimulators of ceramide production, including FasL, PI, Bis, Buty, and Ars, significantly increased cellular ceramide levels in CAECs com-

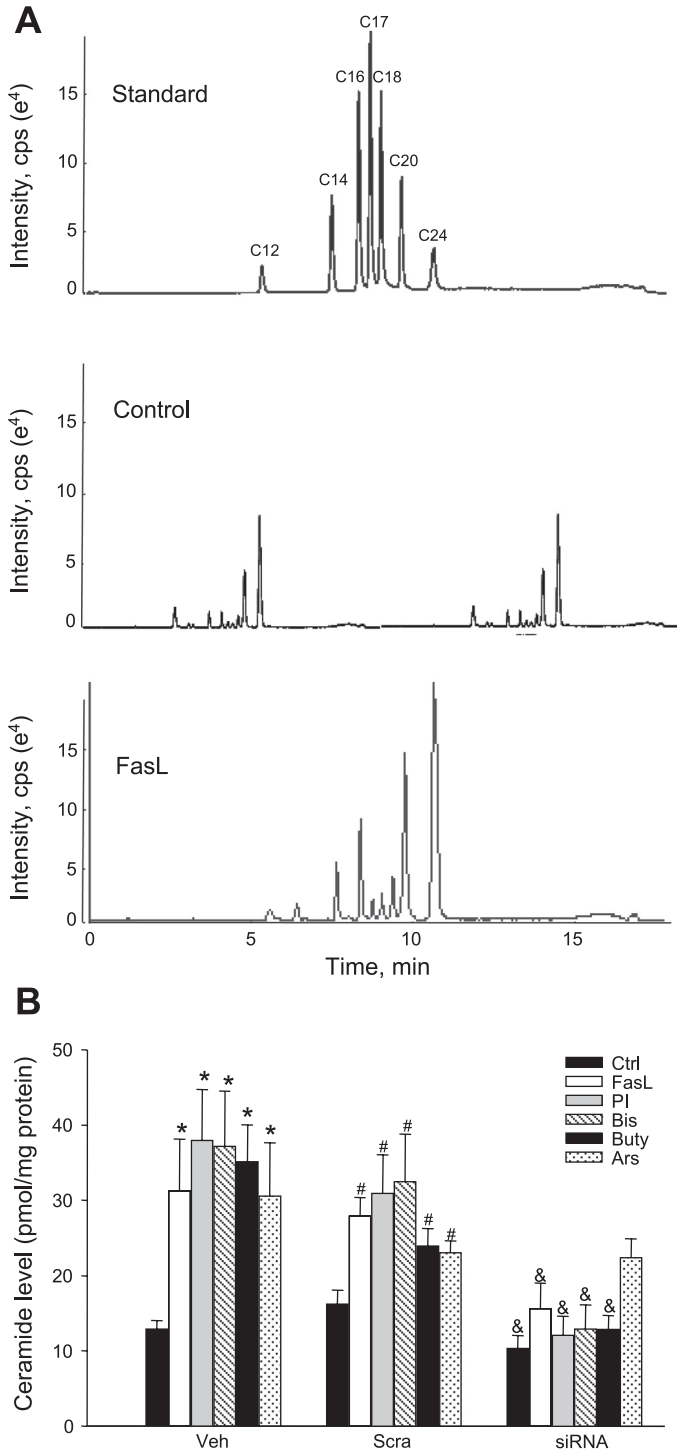

Fig. 2. *A*: representative multiple reaction monitoring chromatography of ceramides separated by liquid chromatography-electrospray ionization-tandem mass spectrometry. cps, Counts per second. *B*: summarized results of ceramide production in Veh, scramble small RNA (sRNA) transfected (Scra) and acid sphingomyelinase (ASM) small interfering RNA (siRNA) transfected cells. Values are means ± SE; $n = 8$ experiments. $^{*}P < 0.05$ vs. Ctrl in Veh-treated cells. $^{\#}P < 0.05$ vs. Ctrl in Scra cells. $^{\&}P < 0.05$ vs. Scra cells with the same treatments.

pared with control cells. In ASM siRNA-transfected cells, however, FasL, PI, Bis, and Buty, but not Ars, failed to increase ceramide production. This was consistent with the fact that Ars mainly activates de novo synthesis of ceramide.

FRET between Lamp1 and LR component. To determine the involvement of lysosomes in LR clustering, we further examined the possible translocation of lysosome-specific markers in LR clusters. As shown in Fig. 3*A*, FRET as the most accurate parameter showing molecular proximity was detected by confocal microscopy between a fluorophore pair, FITC as donor and TRITC as acceptor, which shares the character to allow FRET. The CAECs were costained with FITC-Lamp1 and TRITC-CTXB and underwent an acceptor bleaching protocol. Both pre- and postbleaching images are presented in the *top* and *middle* panels of Fig. 3*A*. FRET image was in the *bottom* panel (in blue), which was generated by subtraction of fluorescent intensity in the prebleaching image from that in postbleaching. Overlaid images showed the colocalization of both Lamp1 and CTXB detected under different protocols. As shown in the FRET image (blue), there was very low FRET detected under control condition (Ctrl). FasL, PI, Bis, and Buty, but not Ars, remarkably increased FRET intensity (blue on the *bottom* panels), demonstrating an energy transfer between lysosomal marker Lamp1, and LR component GM1 ganglioside. Figure 3*B* summarized calculated FRET efficiency from these experiments. FasL, PI, Bis, and Buty increased the FRET efficiency significantly compared with control level, which were from 4.92 to 19.53, 14.11, 14.48, and 19.05%, respectively. The FRET efficiency in Ars-stimulated cells was 6.07%, which was not significant from that measured in control cells. However, when CAECs were pretreated with vacuolin-1, a lysosome fusion inhibitor, the increased FRET efficiency induced by FasL, PI, Bis, and Buty was substantially blocked, suggesting that increased FRET between lysosomal molecules and membrane LRs is associated with lysosomal fusion to the cell membrane.

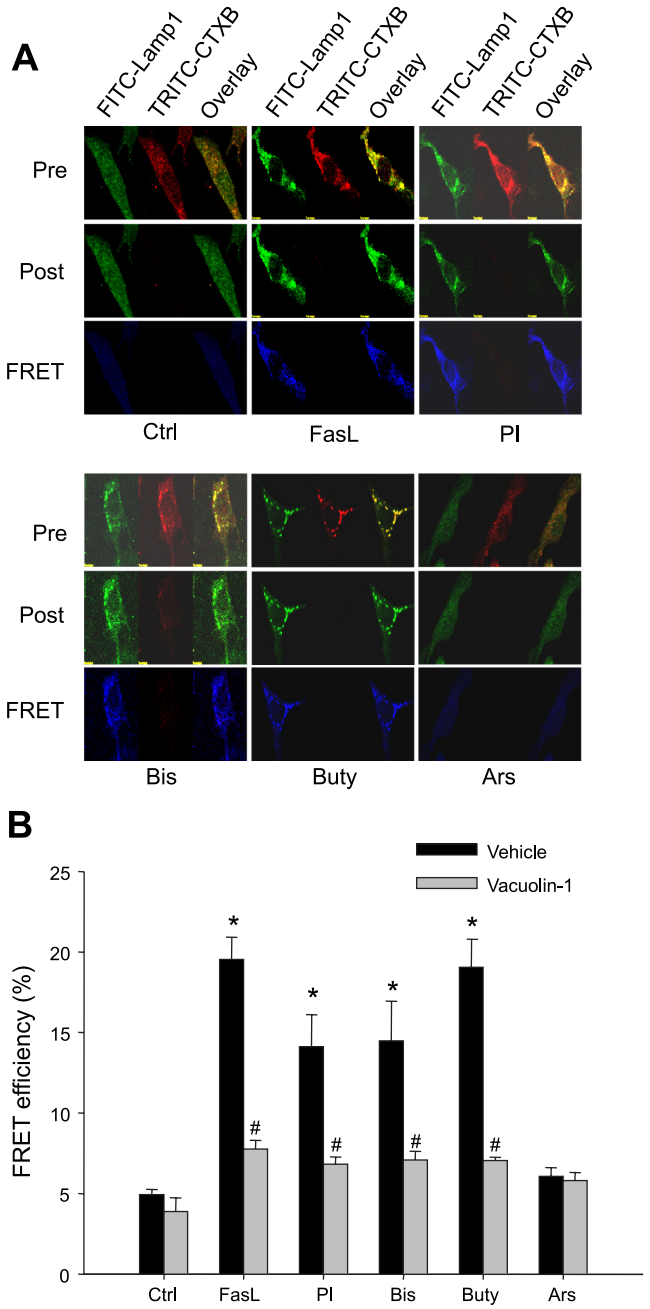

Fig. 3. *A*: representative images of fluorescence resonance energy transfer (FRET) analysis between FITC-Lamp1 and tetramethylrhodamine isothiocyanate cholera toxin B (TRITC-CTXB) in CAECs. Pre and Post, pre- and postbleaching, respectively. *B*: summarized results of detected FRET efficiency between Lamp1 and CTXB in Veh or vacuolin-1 (10 μM for 1 h) pretreated cells. Values are means ± SE; $n = 5$ batches of cells. *$P < 0.05$ vs. Ctrl group. #$P < 0.05$ vs. respective Veh group.

Colocalization of Lamp1 with ASM or ceramide within CAECs. To address possible concern about existence of lysosomal molecules on the cell membrane of CAECs without stimulations, we carefully colocalized these molecules in intact and permeabilized cells. As shown in Fig. 4, CAECs were costained by a FITC-conjugated anti-Lamp1 antibody and TR-conjugated anti-ASM or ceramide antibody (TR-ASM or TR-ceramide). In intact cells, both FITC and TR staining were weak, and there was no significant colocalization of Lamp1 and ASM or ceramide, suggesting that expression of both molecules in the cell membrane, if any, is not colocalized. However, when CAECs were permeabilized with 0.5% Tween 20 for 15 min, both FITC and TR stainings were strengthened as punctuate dots or spots, and both molecules were colocalized, as shown in intensive yellow dots in overlaid images. This tells us that, in control cells, ASM and ceramide were mainly located in lysosomes. When these cells were stimulated by ASM activators or inducers, detection of colocalization of Lamp1 or ASM in the cell membrane, as shown in overlaid images of Fig. 3, represents incorporation of these molecules into the cell membrane by lysosome fusion.

Lysosome fusion induced by FasL and activation of ASM. To directly observe lysosome movement and fusion, three different protocols were performed, including lysosomal FM1–43 quenching and dequenching, as well as FM2–10 destaining. Figure 5 shows the results of FM1–43 quenching. In these experiments, cells were loaded with 8 μM FM1–43, and then 1 mM BPB was added to extracellular solution before any treatments. Since FM1–43 is in lysosomes, unless lysosomes fuse with the cell membrane, BPB could not have access to quench FM1–43. Therefore, detection of FM1–43 fluorescence quenching by BPB indicates lysosome fusion. Fluorescent image and recordings in Fig. 5*A* and *movie 1–3* in the supplemental data depict that PI, but not Ars, induced a

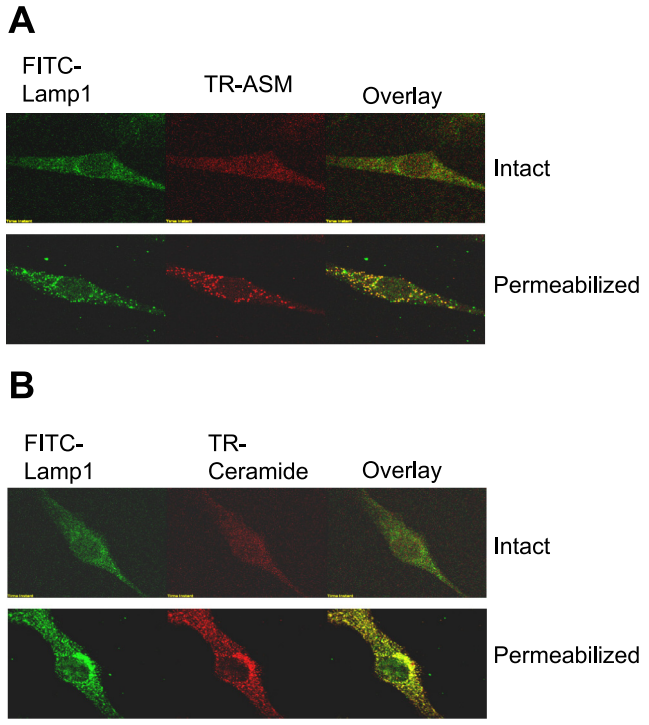

Fig. 4. Colocalization of Lamp1 and ASM (*A*) or ceramide (*B*) detected by confocal microscopy in intact and permeabilized CAECs. FITC-Lamp1 was shown as green fluorescence on the *left*; Texas red (TR)-ASM or ceramide shown red in the *middle*; and overlaid images are on the *right*. Yellow spots in overlaid images indicated colocalization of Lamp1 and ASM or ceramide.

significant FM1–43 quenching. Figure 5*B* summarized results from all different treatments. FasL, PI, and Bis caused a maximal decrease in lysosomal FM1–43 fluorescence by 58.1, 67.5, and 61.6%, respectively, which were more significant than 13.3% of control cells. The decrease in fluorescence induced by Buty and Ars did not show a significant difference compared with that in control cells. Pretreatment of these cells with vacuolin-1 significantly reversed the decrease in fluorescence in FasL-, PI-, and Bis-stimulated cells.

Figure 6 shows the results from dequenching experiments in which lysosomes of CAECs were loaded simultaneously with 8 μM FM1–43 and 1 mM BPB for 2 h and then underwent different treatments. Given the fact that BPB may flow out of lysosome much easier compared with FM1–43, membrane fusion of lysosome could lead to a fast loss of BPB, resulting in FM1–43 dequenching. Therefore, the increase and then decrease of fluorescence under such conditions indicates lysosome fusion. Indeed, as shown in Fig. 6*A* and *movie 4* in the supplemental data, FasL, PI, and Bis first caused an increase in FM1–43 fluorescence followed by a decrease of it. As summarized in Fig. 6*B*, the maximal increases in FM1–43 fluorescence induced by FasL, PI, and Bis were 55.9, 52.1, and 53.5%, respectively. However, Buty and Ars had no significant effect on FM1–43 fluorescence compared with control group. Moreover, when CAECs were pretreated by vacuolin-1, FM1–43 dequenching by FasL, PI, and Bis was almost blocked.

Another method to determine lysosome fusion was to observe destaining of lysosomal dye FM2–10 under confocal microscopy. Figure 7 presents the results from these experiments. In Fig. 7*A*, typical FM2–10 fluorescence destaining was observed in CEACs treated with FasL and PI. The summarized data are presented in Fig. 7*B*. FasL, PI, and Bis, but not Buty and Ars, caused a significant decrease in FM2–10 fluorescence by 49.5, 51.9, and 42.5%, respectively, compared with control level. Pretreatment of the cells with vacuolin-1 blocked the decrease in FM2–10 fluorescence induced by FasL, PI, and Bis.

Blockade of ASM activator-induced LRs clustering and lysosome fusion by silencing of ASM gene. To further clarify the ASM activation-induced LR clustering and lysosome fusion, we silenced the ASM gene and examined the LR patch formation and quenching and dequenching of FM1–43 fluorescence after PI or Bis treatment. As shown in Fig. 8*A*, on the scramble sRNA-transfected cell, PI and Bis induced the LR clustering substantially, which was not present on the ASM siRNA transfected cell. Figure 8*B* shows the results of FM1–43 quenching experiments, depicting that, on the scrambled sRNA transfected cells, PI and Bis decrease FM1–43 fluorescence significantly, and this effect was abolished in ASM siRNA transfected cells. Figure 8*C* presents the results of FM1–43 dequenching experiments. On the scrambled sRNA-, but not ASM siRNA-transfected cells, FM1–43 fluorescence was increased significantly after both PI and Bis treatments.

Inhibition of lysosome function or lysosome fusion reversed FasL, PI, and Bis-induced impairment of endothelium-dependent vasodilation. Endothelium-dependent vasodilation induced by BK was determined in isolated small bovine coronary arteries before and after treatment of FasL, PI, and Bis. Figure 9 shows that BK produced a concentration-dependent relaxation in these small coronary arteries. Incubation of the arteries with FasL, PI, and Bis markedly attenuated the vasodilator response by 36.7, 51.9, and 42.8%, respectively. This attenuation of vasodilator response induced by FasL, PI, and Bis could be reversed by both Baf and vacuolin-1; Baf is a specific inhibitor of vacuolar proton ATPase, which can increase the pH value in lysosomes and disrupt lysosome function.

DISCUSSION

Using confocal microscopy and FRET analysis, the present study first demonstrated that, like a typical stimulator of LR clustering, FasL, activation of ASM by PI and Bis, or induction of ASM expression by Buty induced the formation of LR clusters in CAECs. However, increase in de novo synthesis of ceramide had no such action. Then we used three different measurements, including lysosomal FM1–43 quenching or dequenching and FM1–20 destaining, and confirmed that activation of ASM led to lysosome fusion to the cell membrane, which triggered LR clustering to form signaling platforms or macrodomains. Both silencing the ASM gene and pretreatment with vacuolin-1, a lysosome fusion inhibitor, were found to block LR clustering and membrane proximal lysosome fusion induced by activation of ASM. Functionally, activation of ASM by PI and Bis was demonstrated to impair endothelium-dependent vasodilation in small coronary arteries, which was dependent on lysosome fusion because vacuolin-1 could block such a detrimental effect induced by ASM activation in the intact endothelium of isolated perfused coronary arteries. These results support the view that ASM activation acts as a triggering mechanism or driving force for membrane proximal lysosome fusion to

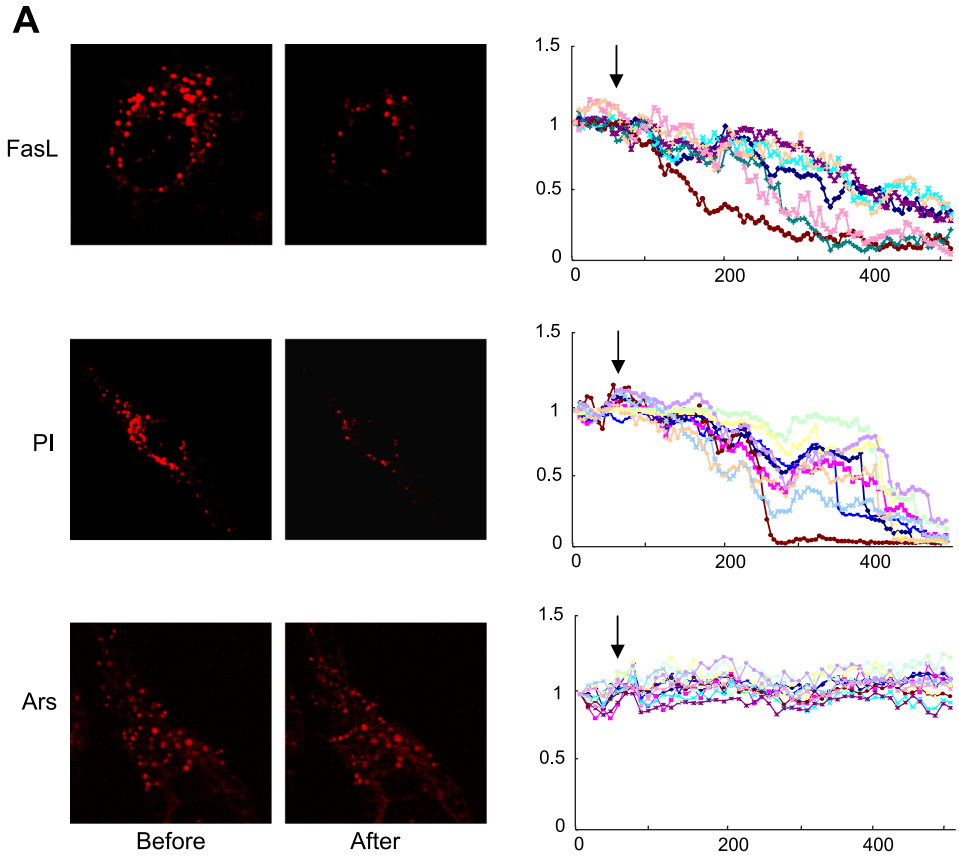

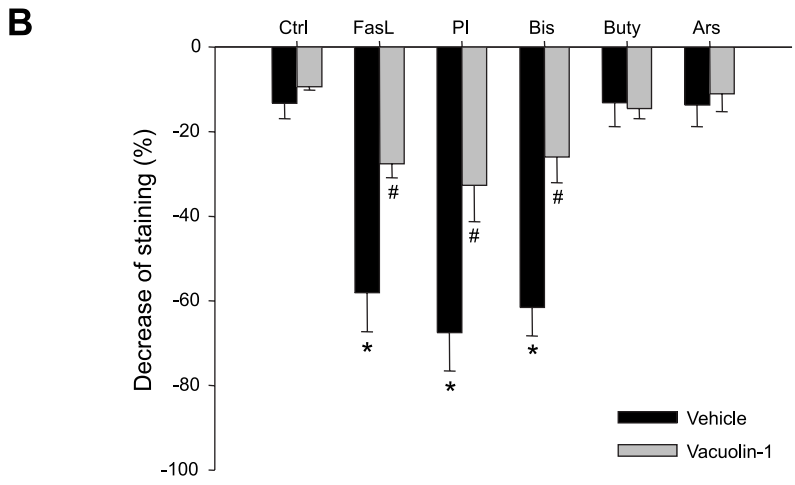

Fig. 5. *A*: representative images and traces before and after treatment with FasL, PI, and Ars in CAECs loaded with 8 μM FM1–43 and in the presence of 1 mM bromide phenol blue (BPB). The arrow shows the beginning of treatments. The fluorescence at 7 min after treatment was read for statistics. *B*: summarized results showing changes of FM1–43 fluorescence in Veh or vacuolin-1 (10 μM for 1 h) pretreated group, normalized by the fluorescence obtained before treatment. Values are means ± SE; $n = 80$ puncta from 5 batches of cells. *$P < 0.05$ vs. Ctrl group. #$P < 0.05$ vs. respective Veh group.

the cell membrane, which may lead to the formation of LR macrodomains regulating endothelial function.

In previous studies, LR clustering to form membrane signaling platforms or macrodomains, in particular, ceramide-enriched macrodomains, has been demonstrated to be associated with activation of ASM (6, 35, 40, 41). Recently, our laboratory has reported that such activated ASM is mainly derived from lysosomes in response to different stimuli, such as FasL and endostatin (18–20). It is generally accepted that activation of ASM in response to any agonists or extracellular stimuli correlates with a translocation of the enzyme from intracellular stores onto the extracellular leaflet of the cell membrane. The ASMs localized in lysosomes are mobilized on stimulation to fuse with the cell membrane. Such fusion results in exposure of ASM onto the outer leaflet of the cell membrane and brings the enzyme in close vicinity to its substrate sphingomyelin and produces ceramide with a very rapid process within 5 s when cells are stimulated (14, 19). According to this working model, lysosomes or acid vesicles are first fused into the cell membrane, and, therefore, ASM incorporated there and was activated, inducing the formation of LR macrodomains. However, this hypothesis has never been confirmed, which is the focus of the present study.

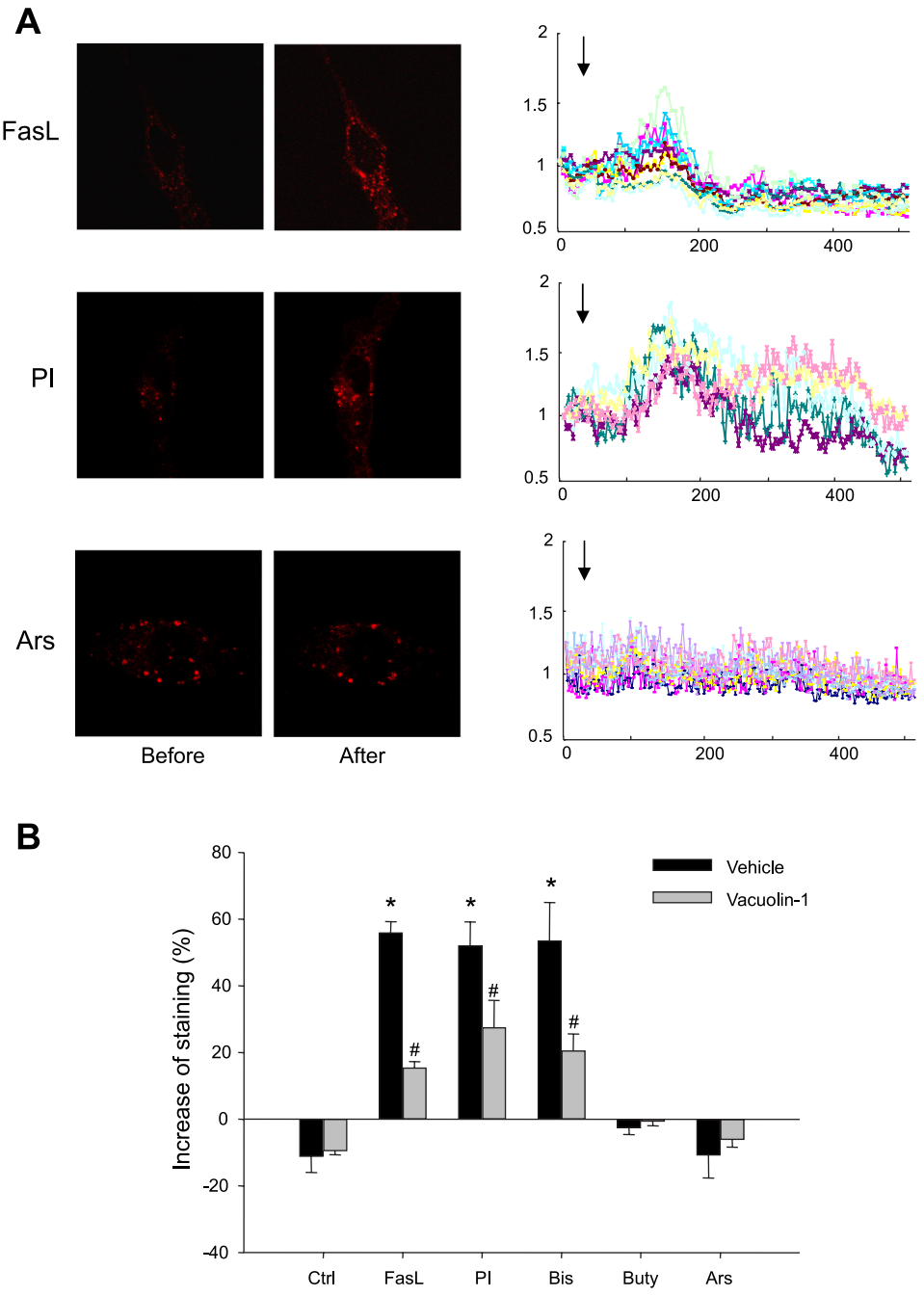

Fig. 6. *A*: representative images and traces before and after treatment with FasL, PI, and Ars in CAECs loaded simultaneously with 8 μM FM1–43 and 1 mM BPB. The arrow shows the beginning of treatments. The highest level of fluorescence (2–3 min after treatment) was read for statistics. *B*: summarized results showing changes of FM1–43 fluorescence in Veh or vacuolin-1 (10 μM for 1 h) pretreated group, normalized by the fluorescence obtained before treatment. Values are means ± SE; $n = 80$ puncta from 5 batches of cells. *$P < 0.05$ vs. Ctrl group. #$P < 0.05$ vs. respective Veh group.

Surprisingly, we demonstrated that direct activation of ASM could trigger membrane proximal lysosome fusion to the cell membrane in CAECs, which challenges the previous assumption that lysosome fusion leads to ASM activation. Using PI and Bis as negatively charged lysosome occurring lipids to stimulate the activity of ASM (25), or an ASM inducer, Buty (37), we found that LR clustering occurred in a manner similar to stimulation by FasL, a strong LR clustering stimulator through activation of its receptors, as shown in our laboratory's previous studies (12, 41). This clustering was shown by detection of LR patches on the cell membrane of CAECs and FRET analysis of lysosomal protein Lamp1 and cell membrane LR marker GM1. However, in the presence of vacuolin-1, a lysosome fusion inhibitor, these ASM activators or inducer failed to produce LR clustering, although they could induce ceramide production, as shown in LC-ESI-MS-MS analysis. On the other hand, Ars as an inducer of de novo synthesis of ceramide or inhibitor of glucosylceramide synthase activity (7) could not enhance LR clustering, although it increased ceramide production at the similar potency to PI, Bis, and Buty. These results suggest that ceramide production due to activation of ASM, but not to increase in de novo synthesis, causes LR clustering, which is a process dependent on lysosome fusion. It seems that ASM may first be activated, and then membrane proximal lysosome fusion into the cell membrane occurs, thereby resulting in LR clustering.

To further test this hypothesis, we directly detected membrane proximal lysosome fusion in CAECs during activation of

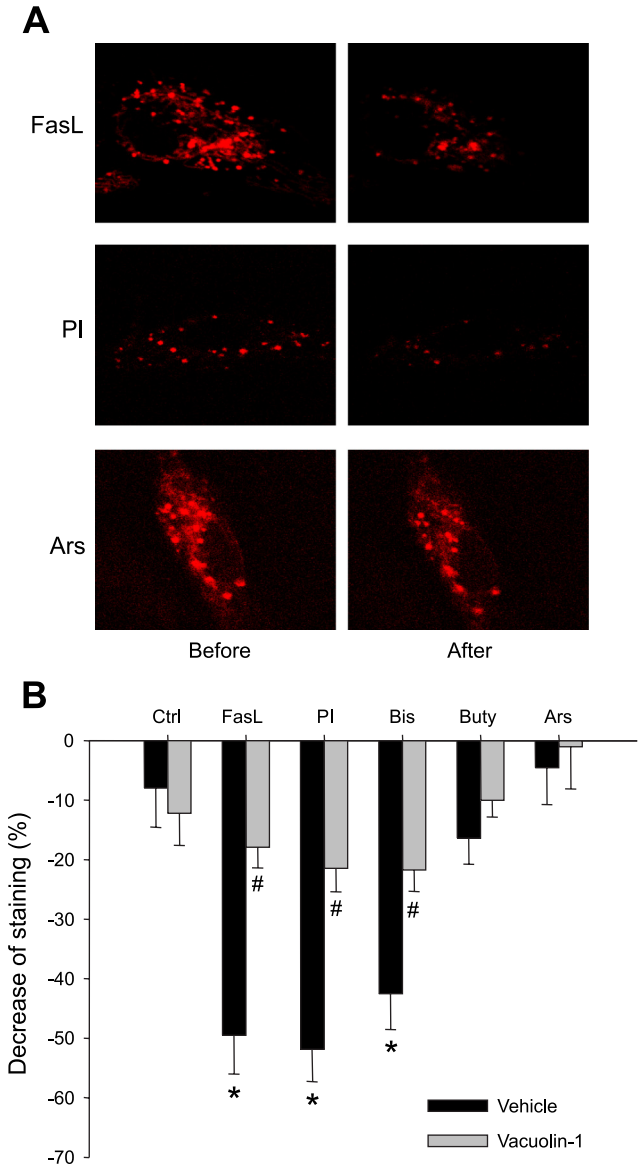

Fig. 7. *A*: representative images before and after treatment with FasL, PI, and Ars in CAECs loaded with 100 μM FM2–10. The fluorescence at 7 min after treatment was read for statistics. *B*: summarized results showing changes of FM2–10 fluorescence in Veh or vacuolin-1 (10 μM for 1 h) pretreated group, normalized by the fluorescence obtained before treatment. Values are means ± SE; $n = 80$ puncta from 5 batches of cells. *$P < 0.05$ vs. Ctrl group. #$P < 0.05$ vs. respective Veh group.

ASM. Fluorescent dye FM1–43 or FM2–10 was first loaded into lysosomes, and then FM1–43 quenching or dequenching by BPB or FM2–10 destaining due to lysosome fusion were dynamically observed over 30–60 min under a confocal microscope. These methods for observation of lysosome fusion into the cell membrane were confirmed to be specific and efficient in our laboratory's previous studies (19) and by others (23, 42). It was found that the activators of ASM, PI, and Bis induced both quenching and dequenching of FM1–43, as well as destaining of FM2–10, and the vacuolin-1 almost completely blocked such effect of PI and Bis. This provides direct evidence that activation of ASM may drive membrane proximal lysosomes to fuse into the cell membrane and thereby produce downstream LR clustering and signaling. In these experiments, we could not observe that induction of ASM by Buty and activation of ceramide by de novo synthesis produced lysosome fusion in CAECs. The failure of Buty to induce lysosome fusion might be due to a relatively longer time needed for ASM expression to be regulated.

To further verify that the observed LR clustering and membrane proximal lysosome fusion were through ASM activation instead of other ASM unconcerned mechanisms, we first si-

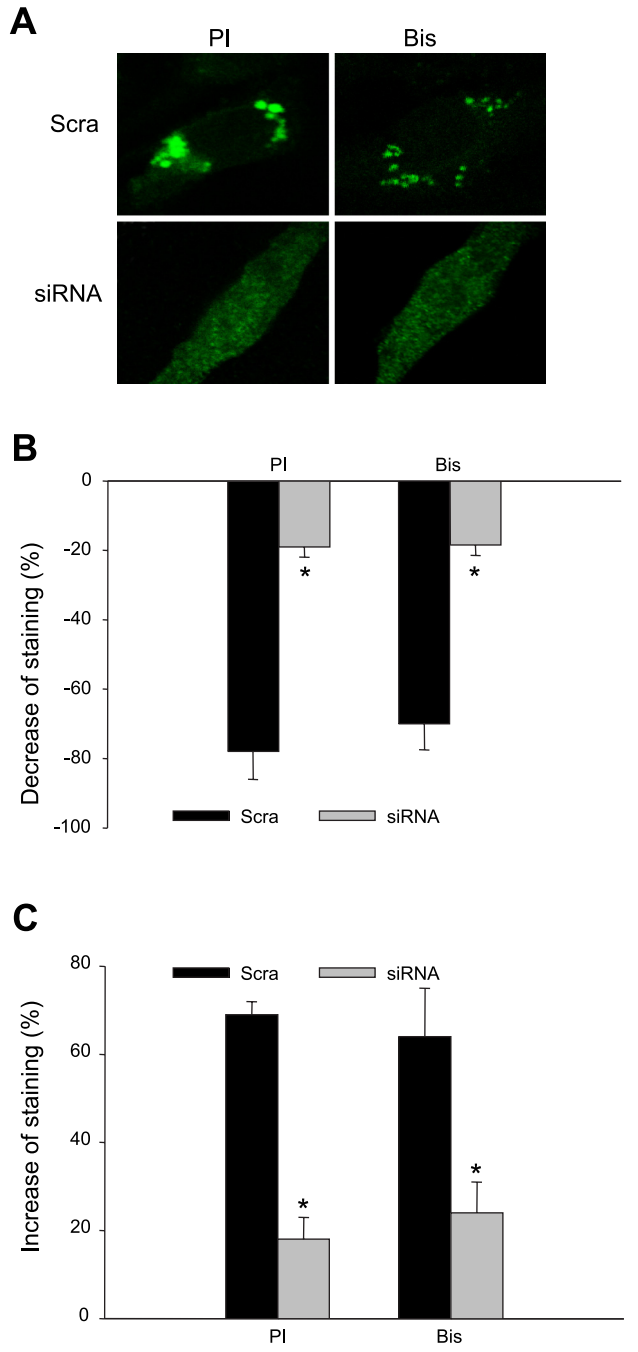

Fig. 8. *A*: representative images of LR clustering (*A*) induced by PI (5 μg/ml for 30 min) and Bis (1 μg/ml for 30 min) in Scra or ASM siRNA transfected cells. Summarized results showing quenching (*B*) and dequenching (*C*) of FM1–43 fluorescence in Scra- and siRNA-treated cell group. Values are means ± SE; $n = 80$ puncta from 5 batches of cells. *$P < 0.05$ vs. Scra group.

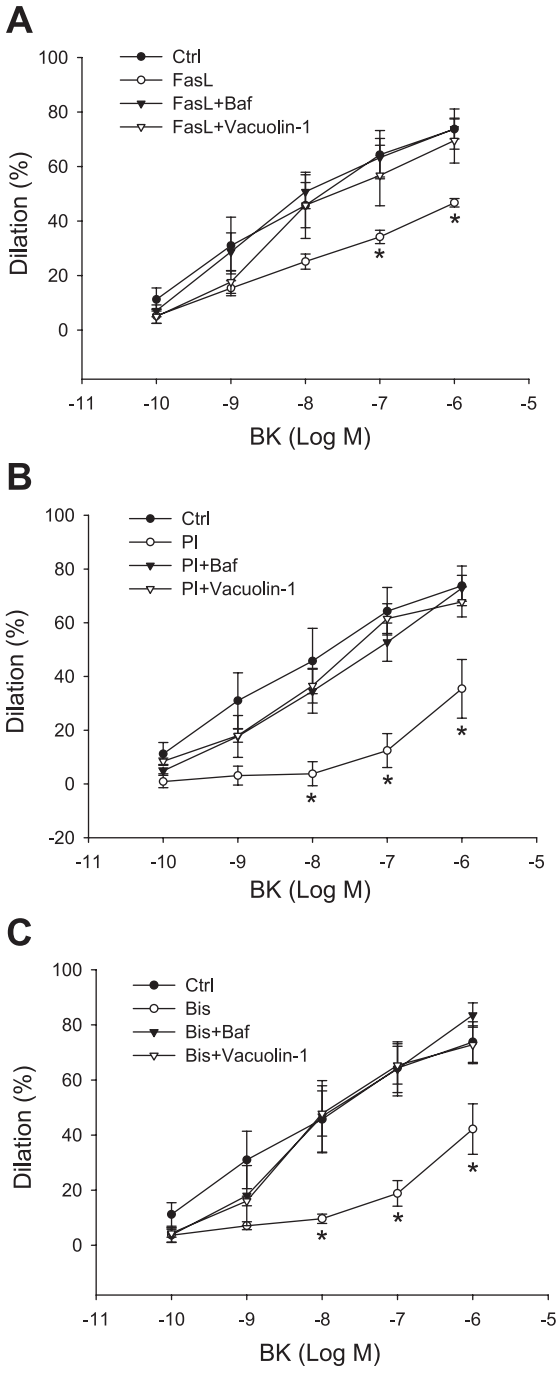

Fig. 9. Impairment of endothelium-dependent vasodilator response to bradykinin (BK) induced by FasL (*A*), PI (*B*), and Bis (*C*) in small coronary arteries before and after application of bafilomycine (Baf; 100 nM for 20 min) and vacuolin-1 (10 μM for 1 h). Values are means ± SE; $n = 5$ cow hearts. *$P <$ 0.05 vs. Ctrl group.

lenced the ASM expression in cells and then examined the effect of ASM activators. The results show that ASM siRNA could markedly reverse the LR clustering and membrane proximal lysosome fusion induced by ASM activators. This further supports our view that ASM activation acts as a crucial driving force for the lysosome fusion and LR clustering.

Our findings in the present study provide a new working model, which may mediate LR clustering and formation of LR signaling platforms in arterial ECs. This model emphasizes that ceramide produced due to activation of ASM leads to membrane proximal lysosome fusion into the cell membrane and thereby results in LR clustering, promoting transmembrane signaling by aggregation or translocation of signal molecules in or around LRs. This demonstrates a novel function of lysosomes in the mediation of transmembrane signaling in vascular ECs. In this regard, previous studies have also reported that ASM, by generation of ceramide, enhances the fusogenicity of cellular membranes at the intra- and intercellular level. Although ASM seems not to be critical for the generation of the fusion pore per se, it contributes to the widening of the initial fusion, as would be required for the merging of lysosomes with a phagosome in macrophages. Under this condition, ceramide is confined to the membranes of phagosomes and lysosomes or the extracellular leaflet of the plasma membrane. It has been suggested that ASM regulates vesicular fusion processes by modifying the steric conformation of cellular membranes (36). This ceramide-mediated lysosome fusion was also found to mediate acrosomal exocytosis in boar spermatozoa stimulated by Ca^{2+}/A23187. It was concluded that ceramide itself rather than its metabolites may play a role in the sequence of events leading to membrane fusion of acrosomes (26). In addition, several studies about CD95 (Fas) and cell apoptosis demonstrated that ceramide is able to promote membrane fusion. Treatment of cells with sphingomyelinase could induce the formation of endocytic vesicles, and the process is completely ATP independent (34). More similarly, FasL was found to trigger a ceramide-dependent trafficking of intracellularly stored CD95 to cell plasma membrane, thereby amplifying CD95 activation (29). Under this condition, ceramide is formed very rapidly in response to FasL, which leads to CD95 trafficking and thereby clustering in plasma membrane (29). Taken together, it is concluded that ceramide from ASM activation is able to trigger or enhance lysosome fusion into the cell membrane or other organelles and thereby regulate cellular activity.

It should be noted that de novo synthesis of ceramide seems not to be involved in this membrane fusion process. This view was also supported by a report that only hydrolysis of sphingomyelin promotes liposome fusion (2, 10, 11, 17, 30). Failure of the de novo synthesis of ceramide to activate or promote lysosome fusion to the cell membrane may be related to its enzymatic reaction time and location. In general, it is accepted that the *de novo* synthesis of ceramide takes more time in response to any stimuli compared with sphingomyelin hydrolysis (7, 32, 38). In addition, this ceramide de novo synthesis mainly occurs in the endoplasmic reticulum. Ceramide is subsequently transported to the Golgi by either vesicular trafficking or the ceramide transfer protein (CERT). Once in the Golgi apparatus, ceramide can be further metabolized to other sphingolipids, such as back to sphingomyelin or forming a complex glycosphingolipids (15). This synthesis and transport process of ceramide within cells may limit its ability to participate in lysosome fusion to the cell membrane and thereby mediate signaling events.

Another important finding of the present study is that activation of ASM impaired endothelial function through lysosome fusion. Although our previous studies have demonstrated that FasL may induce endothelial dysfunction through activation of ASM, the mechanism mediating such action of ASM is still poorly understood. In the present study, we further clari-

fied that direct activation of ASM by PI or Bis significantly blunted the endothelium-dependent vasodilator response to BK. Lysosome function inhibition by Baf and fusion blockade by vacuolin-1 could substantially attenuate such damaging effects induced by activation of ASM or FasL stimulation on endothelial function. To our knowledge, these results for the first time demonstrate that inhibition of lysosome fusion is of importance in protecting ECs from death receptor activation and subsequent signaling cascade, such as ASM activation. Such experimental evidence may suggest lysosome fusion through ASM activation as a new therapeutic target for protection of endothelial function in coronary circulation. We did not attempt to test the effect of the de novo synthesis of ceramide on endothelial function in intact vessels, for we found that this type of ceramide production did participate in the membrane proximal lysosome fusion and LR clustering in coronary ECs. However, the de novo ceramide synthesis may lead to cell apoptosis, if the incubation time was long enough (7, 38), which may also contribute to endothelial dysfunction or injury, although this action of ceramide may not be associated with LR clustering and LR-redox platform formation.

It should be noted that the present study did not preclude the possibility of ASM-dependent but ceramide-unrelated mechanism to play a role in membrane proximal lysosome fusion and LR clustering, given that the de novo synthesis of ceramide seemed not be involved in the process. Further study intending to examine LR cluster formation and membrane proximal lysosome fusion by depleting sphingomyelin from cell membrane may be needed to clarify this issue. However, such specific depletion of sphingomyelin without damage of cell function is so far not yet possible.

In summary, the present study demonstrated that ASM activation promoted LR clustering as stimulation of death receptors, such as Fas did. The mechanism mediating this ASM-induced LR clustering was related to ceramide production in lysosomes and consequent membrane proximal lysosome fusion to the plasma membrane. Inhibition of lysosome function or lysosome fusion restored endothelium-dependent vasodilation impaired by FasL and ASM activation. Our results indicate ASM activation to produce ceramide is a triggering factor or driving force for membrane proximal lysosome fusion to the cell membrane in CAECs in response to death receptor activator, such as FasL. This lysosome fusion mechanism in mediating or promoting endothelial dysfunction may be of importance in the development of new therapeutic strategies in prevention or treatment of vascular diseases, such as atherosclerosis, diabetic vasculopathy, or hypertension.

GRANTS

This study was supported by National Heart, Lung, and Blood Institute Grants HL-57244, HL-75316, and HL-091464.

DISCLOSURES

I am not aware of financial conflict(s) with the subject matter or materials discussed in this manuscript with any of the authors, or any of the authors' academic institutions or employers.

REFERENCES

1. **Allen JA, Halverson-Tamboli RA, Rasenick MM.** Lipid raft microdomains and neurotransmitter signalling. *Nat Rev Neurosci* 8: 128–140, 2007.
2. **Basanez G, Ruiz-Arguello MB, Alonso A, Goni FM, Karlsson G, Edwards K.** Morphological changes induced by phospholipase C and by sphingomyelinase on large unilamellar vesicles: a cryo-transmission electron microscopy study of liposome fusion. *Biophys J* 72: 2630–2637, 1997.
3. **Bollinger CR, Teichgraber V, Gulbins E.** Ceramide-enriched membrane domains. *Biochim Biophys Acta* 1746: 284–294, 2005.
4. **Brandin L, Bergstrom G, Manhem K, Gustafsson H.** Oestrogen modulates vascular adrenergic reactivity of the spontaneously hypertensive rat. *J Hypertens* 21: 1695–1702, 2003.
5. **Bund SJ, Lee RM.** Arterial structural changes in hypertension: a consideration of methodology, terminology and functional consequence. *J Vasc Res* 40: 547–557, 2003.
6. **Cremesti AE, Goni FM, Kolesnick R.** Role of sphingomyelinase and ceramide in modulating rafts: do biophysical properties determine biologic outcome? *FEBS Lett* 531: 47–53, 2002.
7. **Dbaibo GS, Kfoury Y, Darwiche N, Panjarian S, Kozhaya L, Nasr R, Abdallah M, Hermine O, El-Sabban M, de The H, Bazarbachi A.** Arsenic trioxide induces accumulation of cytotoxic levels of ceramide in acute promyelocytic leukemia and adult T-cell leukemia/lymphoma cells through de novo ceramide synthesis and inhibition of glucosylceramide synthase activity. *Haematologica* 92: 753–762, 2007.
8. **Fillet M, Van Heugen JC, Servais AC, De Graeve J, Crommen J.** Separation, identification and quantitation of ceramides in human cancer cells by liquid chromatography-electrospray ionization tandem mass spectrometry. *J Chromatogr A* 949: 225–233, 2002.
9. **Fullekrug J, Simons K.** Lipid rafts and apical membrane traffic. *Ann N Y Acad Sci* 1014: 164–169, 2004.
10. **Goni FM, Alonso A.** Biophysics of sphingolipids. I. Membrane properties of sphingosine, ceramides and other simple sphingolipids. *Biochim Biophys Acta* 1758: 1902–1921, 2006.
11. **Goni FM, Alonso A.** Membrane fusion induced by phospholipase C and sphingomyelinases. *Biosci Rep* 20: 443–463, 2000.
12. **Grassme H, Jekle A, Riehle A, Schwarz H, Berger J, Sandhoff K, Kolesnick R, Gulbins E.** CD95 signaling via ceramide-rich membrane rafts. *J Biol Chem* 276: 20589–20596, 2001.
13. **Grassme H, Riethmuller J, Gulbins E.** Biological aspects of ceramide-enriched membrane domains. *Prog Lipid Res* 46: 161–170, 2007.
14. **Gulbins E, Li PL.** Physiological and pathophysiological aspects of ceramide. *Am J Physiol Regul Integr Comp Physiol* 290: R11–R26, 2006.
15. **Hannun YA, Obeid LM.** Principles of bioactive lipid signalling: lessons from sphingolipids. *Nat Rev Mol Cell Biol* 9: 139–150, 2008.
16. **Harata NC, Choi S, Pyle JL, Aravanis AM, Tsien RW.** Frequency-dependent kinetics and prevalence of kiss-and-run and reuse at hippocampal synapses studied with novel quenching methods. *Neuron* 49: 243–256, 2006.
17. **Hinkovska-Galcheva VT, Boxer LA, Mansfield PJ, Harsh D, Blackwood A, Shayman JA.** The formation of ceramide-1-phosphate during neutrophil phagocytosis and its role in liposome fusion. *J Biol Chem* 273: 33203–33209, 1998.
18. **Jin S, Yi F, Li PL.** Contribution of lysosomal vesicles to the formation of lipid raft redox signaling platforms in endothelial cells. *Antioxid Redox Signal* 9: 1417–1426, 2007.
19. **Jin S, Yi F, Zhang F, Poklis JL, Li PL.** Lysosomal targeting and trafficking of acid sphingomyelinase to lipid raft platforms in coronary endothelial cells. *Arterioscler Thromb Vasc Biol* 28: 2056–2062, 2008.
20. **Jin S, Zhang Y, Yi F, Li PL.** Critical role of lipid raft redox signaling platforms in endostatin-induced coronary endothelial dysfunction. *Arterioscler Thromb Vasc Biol* 28: 485–490, 2008.
21. **Kenworthy AK, Petranova N, Edidin M.** High-resolution FRET microscopy of cholera toxin B-subunit and GPI-anchored proteins in cell plasma membranes. *Mol Biol Cell* 11: 1645–1655, 2000.
22. **Kinoshita A, Fukumoto H, Shah T, Whelan CM, Irizarry MC, Hyman BT.** Demonstration by FRET of BACE interaction with the amyloid precursor protein at the cell surface and in early endosomes. *J Cell Sci* 116: 3339–3346, 2003.
23. **Klingauf J, Kavalali ET, Tsien RW.** Kinetics and regulation of fast endocytosis at hippocampal synapses. *Nature* 394: 581–585, 1998.
24. **Li PL, Zhang Y, Yi F.** Lipid raft redox signaling platforms in endothelial dysfunction. *Antioxid Redox Signal* 9: 1457–1470, 2007.
25. **Linke T, Wilkening G, Lansmann S, Moczall H, Bartelsen O, Weisgerber J, Sandhoff K.** Stimulation of acid sphingomyelinase activity by lysosomal lipids and sphingolipid activator proteins. *Biol Chem* 382: 283–290, 2001.

26. **Murase T, Imaeda N, Kondoh N, Tsubota T.** Ceramide enhances acrosomal exocytosis triggered by calcium and the calcium ionophore A23187 in boar spermatozoa. *J Reprod Dev* 50: 667–674, 2004.
27. **Natoli G, Costanzo A, Guido F, Moretti F, Levrero M.** Apoptotic, non-apoptotic, and anti-apoptotic pathways of tumor necrosis factor signalling. *Biochem Pharmacol* 56: 915–920, 1998.
28. **Nieminen J, Kuno A, Hirabayashi J, Sato S.** Visualization of galectin-3 oligomerization on the surface of neutrophils and endothelial cells using fluorescence resonance energy transfer. *J Biol Chem* 282: 1374–1383, 2007.
29. **Reinehr R, Haussinger D.** CD95 ligation and intracellular membrane flow. *Biochem J* 413: e11–e12, 2008.
30. **Ruiz-Arguello MB, Basanez G, Goni FM, Alonso A.** Different effects of enzyme-generated ceramides and diacylglycerols in phospholipid membrane fusion and leakage. *J Biol Chem* 271: 26616–26621, 1996.
31. **Schramm M, Herz J, Haas A, Kronke M, Utermohlen O.** Acid sphingomyelinase is required for efficient phago-lysosomal fusion. *Cell Microbiol* 10: 1839–1853, 2008.
32. **Seumois G, Fillet M, Gillet L, Faccinetto C, Desmet C, Francois C, Dewals B, Oury C, Vanderplasschen A, Lekeux P, Bureau F.** De novo C16- and C24-ceramide generation contributes to spontaneous neutrophil apoptosis. *J Leukoc Biol* 81: 1477–1486, 2007.
33. **Silvius JR, Nabi IR.** Fluorescence-quenching and resonance energy transfer studies of lipid microdomains in model and biological membranes. *Mol Membr Biol* 23: 5–16, 2006.
34. **Soreghan B, Thomas SN, Yang AJ.** Aberrant sphingomyelin/ceramide metabolic-induced neuronal endosomal/lysosomal dysfunction: potential pathological consequences in age-related neurodegeneration. *Adv Drug Deliv Rev* 55: 1515–1524, 2003.
35. **Touyz RM.** Lipid rafts take center stage in endothelial cell redox signaling by death receptors. *Hypertension* 47: 16–18, 2006.
36. **Utermohlen O, Herz J, Schramm M, Kronke M.** Fusogenicity of membranes: the impact of acid sphingomyelinase on innate immune responses. *Immunobiology* 213: 307–314, 2008.
37. **Wu J, Cheng Y, Jonsson BA, Nilsson A, Duan RD.** Acid sphingomyelinase is induced by butyrate but does not initiate the anticancer effect of butyrate in HT29 and HepG2 cells. *J Lipid Res* 46: 1944–1952, 2005.
38. **Xu J, Yeh CH, Chen S, He L, Sensi SL, Canzoniero LM, Choi DW, Hsu CY.** Involvement of de novo ceramide biosynthesis in tumor necrosis factor-alpha/cycloheximide-induced cerebral endothelial cell death. *J Biol Chem* 273: 16521–16526, 1998.
39. **Yi F, Chen QZ, Jin S, Li PL.** Mechanism of homocysteine-induced Rac1/NADPH oxidase activation in mesangial cells: role of guanine nucleotide exchange factor Vav2. *Cell Physiol Biochem* 20: 909–918, 2007.
40. **Zhang AY, Yi F, Jin S, Xia M, Chen QZ, Gulbins E, Li PL.** Acid sphingomyelinase and its redox amplification in formation of lipid raft redox signaling platforms in endothelial cells. *Antioxid Redox Signal* 9: 817–828, 2007.
41. **Zhang AY, Yi F, Zhang G, Gulbins E, Li PL.** Lipid raft clustering and redox signaling platform formation in coronary arterial endothelial cells. *Hypertension* 47: 74–80, 2006.
42. **Zhang Z, Chen G, Zhou W, Song A, Xu T, Luo Q, Wang W, Gu XS, Duan S.** Regulated ATP release from astrocytes through lysosome exocytosis. *Nat Cell Biol* 9: 945–953, 2007.